Navigating Patterns Analysis for Onboard Guidance Support in Crossing Collision-Avoidance Operations

Baiheng Wu, Guoyuan Li*, Luman Zhao, Hans-Ingar Johansen Aandahl, Hans Petter Hildre, and Houxiang Zhang

Are with the Department of Ocean Operations and Civil Engineering, Norwegian University of Science and Technology, 6009, Ålesund, 6009, Norway.
Email: baiheng.wu@ntnu.no; guoyuan.li@ntnu.no; luman.zhao@ntnu.no; hiaandah@stud.ntnu.no; hans.p.hildre@ntnu.no; hozh@ntnu.no

xxxxxxx

***Abstract*—A proper interpretation and classification of navigators' operational behaviors is crucial to the design of onboard decision-support systems. This research work dives into the study of navigators' navigating patterns (NPs) in a maritime collision-avoidance (CA) traffic situation. Three NPs, specifically conservative, moderate, and aggressive modes, are identified with respect to a collision risk assessment (CRA) by interpreting data collected from the GPS and automatic identification systems. The CRA is realized following the collision risk modeling concept of the closest point of approach. Then, a human-centered onboard guidance-support system is developed according to the patterns identified to help navigators make decisions. This proposed approach is implemented in the scenario of sailing across a narrow strait, where human intelligence remains necessary in the foreseeable future. The research experiment was conducted on Kongsberg maritime simulators. Thirty-six rounds of sailing data containing 108 CA subtasks were collected and analyzed to classify NPs. Afterward, a guidance-support system was designed based on the patterns' demonstration. An additional experiment to test the developed system in the same scenario was organized on the same simulator. The results show that the system can considerably improve the navigator's navigation management ability in CA operations. Our approach combines data analysis and risk modeling with authentic human-operated navigating data and traffic information, which makes it distinct from traditional intuitive and cognitive maritime traffic modeling. It is the first one that defines NPs and puts them into potential industrial application pragmatically**

Digital Object Identifier 10.1109/MITS.2021.3108473
Date of current version: 7 October 2021

*Corresponding author

1939-1390/21©2021IEEE

Intelligent maritime transportation systems (IMTSs) have received great attention in both academia and industry in the past decades [1], [2]. IMTSs are expected to increase maritime transportation efficiency, prevent human-factor-related failures, and reduce the cost of human resources [3], [4]. With increasing data accessibility, the topic of leveraging data to support IMTSs has gained popularity and thus been studied and developed extensively [5]–[7]. In current industrial practice, mainstream data sources include global navigation satellite systems, automatic identification systems (AISs), onboard-equipped inertial measurement units and gyros, and shore-based traffic and environment-sensing infrastructures (including radars and optical/infrared cameras). Data are often reorganized and plotted on onboard graphical interfaces, such as automatic radar plotting aids (ARPAs) and electronic chart display and information systems (ECDISs), to efficiently assist navigators. These data and tools, when well managed and interpreted, can potentially optimize navigating solutions to the major concerns raised in the field of IMTS, such as ship autonomy, traffic surveillance, route planning, transportation scheduling, and so on. (See "Nomenclature" for explanations of the acronyms used throughout.)

The development of ship autonomy for maritime autonomous surface ships (MASS) has been a major topic in IMTSs for decades [8], [56]. Under the influence of the rapid development of advanced control theory and computer sciences, this topic is now experiencing a rejuvenation, and related research has become increasingly systematic. Different parties, including national/international organizations [9], [10], classification societies [11], [12], and research entities [13], [14], have provided their particular insights of the definition and/or interpretation of various levels of MASS. The degrees of MASS identified by the International Maritime Organization (IMO) are listed in Table 1 [9].

According to Table 1, from the manually operated ships to the fully autonomous ships, there are several in-between degrees of the development of ship intelligence. Except for in degree 4 when humans are out of the loop, human controls at different levels over the ship are yet irreplaceable. Current ship intelligence, which is already implemented in maritime industry, is only at degree 1, according to the IMO. This implies that to reach the excellence of MASS, there is still a long way to go. To do so, we should address human–machine-interaction problems as well as the conflicts caused between human knowledge/experience and the developed ship intelligence. In this regard, understanding navigators' behaviors as well as identifying and analyzing their navigating patterns (NPs) is indispensable in accelerating the development of MASS [15].

The key issue that hinders IMTSs and MASS from being fully realized is that maritime conventions and regulations are predominantly qualitative based and lack quantitative approaches on standardized operational practice. For example, in the *Convention on the International Regulations for Preventing Collisions at Sea* (*COLREGs*) [16], it regulates only the conditions quantitatively in which ships are deemed to be caught in a collision risk situation, but it does not give any specific standard for operations in a quantitative way to avoid collision [17]. Basically, *COLREGs* itself is formulated in an intuitive manner as a general guidance for human-centered onboard control; yet, this has brought the following two main issues:

- Navigation trainees usually find *COLREGs* difficult to understand [18]. The decision on the collision-avoidance (CA) operational actions strongly depends on expertise knowledge.
- A qualitative *COLREGs* imposes great challenges on the development and implementation of IMTSs and MASS, regardless of the rule- or algorithm-based approach.

However, for airborne crafts in the aviation industry where operating environment is also unstructured, a series of quantitative CA guidelines has been formulated, together with corresponding operation recommendations [19]. Although waterborne sailing is a relatively low-speed and slow-response process, establishing quantitative guidelines is crucial to develop MASS.

Nomenclature

AIS:	automatic identification system
ARPA:	automatic radar plotting aid
CA:	collision avoidance
CRA:	collision risk assessment
COLREGs:	*Convention on the International Regulations for Preventing Collisions at Sea*
CPA:	closest point of approach (except for the CPA in Figure 13; a specific clarification can be found in the caption for Figure 13)
DCPA:	distance the closest point of approach
ECDIS:	electronic chart display and information system
GNSS:	global navigation satellite systems
HITL:	human in the loop
IMO:	International Maritime Organization
MASS:	maritime autonomous surface ships
NP:	navigating pattern
NPA:	navigating patterns analysis
OS:	own ship
TCPA:	time to the closest point of approach
TS:	target ship.

Table 1. The degrees of autonomy for MASS operations identified by the IMO.

Level	Exercise scope
Degree 1	Ship with automated processes and decision support
Degree 2	Remotely controlled ship with seafarers on board
Degree 3	Remotely controlled ship without seafarers on board
Degree 4	Fully autonomous ship

In this article, we narrow down the research scope to the NPs of navigators when sailing in a narrow strait with intense marine traffic coming from the starboard side of the own ship (OS). This scenario is drawn from traffic environment commonly seen in some busy straits, such as the Dover strait. In these congested waters, there are specific separation schemes to secure the safety and efficiency of the traffic. When a ship is crossing such a strait, usually the target ships (TSs) are coming from either the starboard or portboard side at a time. We summarize navigators' NPs reflected by the recorded maneuvering data and route evaluation in such a traffic environment. Then we use the concluded patterns' features to provide onboard guidance to support navigators.

The following issues are addressed in this article:

- A data-based NP analysis (NPA) method is conceived for a crossing scenario in the CA task, and three NPs, specifically conservative, moderate, and aggressive modes, are concluded and interpreted.
- A guidance-support system is developed based on the NPA to assist navigators in making decisions on sailing routes and CA strategies selection.

Related Work

In this article, we mainly focus on the NPA, but we also cover two other minor subjects: risk assessment and onboard decision support for the CA.

Different from the research progress of NPA in the maritime field, similar topics regarding driving styles have been studied extensively in the field of automobile for decades. Driving styles under different circumstances have been investigated and assessed from various perspectives. They are often classified according to different driving styles, such as aggressive-moderate-conservative, risky-mild-safe, and so forth. [20]–[24]. Similar research interest can also be found in trains operating along railways [25].

Moving back to the maritime field, the research on NPA incorporates with the investigation on human factors. Most of the recent research items are regulated in the framework of human factors analysis and classification system (HFACS) [26], [27]. The human factors affecting navigational safety have been studied from an organizational aspect [28], [29]. In addition to the HFACS framework, a fault-tree analysis is also used to tackle human-related maritime accidents [30]. The Bayesian topology network is also utilized to assess human reliability and risk [31].

A shared characteristic discovered from previous research is that more attention is given to the results and the connected individual events/operations. Another group of researchers put efforts into the operational process study. Instead of discussing the causalities among individual events, they attempt to make a descriptive interpretation over the navigating process. In terms of the research specifically focusing on the NPs and behavioral modeling, progress is also achieved in conceptualization. The idea to quantitatively describe navigators' behaviors and strategies with respect to (w.r.t.) risk assessment index was raised early but lacks abundant data for it to be demonstrated comprehensively [32]. In recent years, scholars have attempted to define NPs; for example, an intuitive classification of patterns, such as chancer (eager to take risk), neutral (conservative), and passive (reluctant to take a risk) in terms of the navigators' attitudes toward potential risks [33]; a qualitative classification, including the hazardous and safe patterns summarized from several types of navigators' behavioral profiles (professional, decisive, risk-taker, careful, and so on.) [34]; and a quantitative evaluation of navigators' maneuvering performance levels, including low-poor, moderate-average, high-excellent, which were realized by analyzing operations' details and ship responses [35].

Different from the automobile field, which has ready access to massive amounts of road data, maritime practitioners adopt similar strategies as in aviation by using realistic simulator cabins to collect human-centered maneuvering data for training and research purposes [36], [37]. Simulator-based data have been used to analyze risk level and human performance in various scenarios [38].

In this research work, we look into CA operation, which is deemed to be one of the most critical operations during sailing. First, regarding policy and convention, CA operation is addressed under *COLREGs*. As problems in the current *COLREGs* were mentioned previously, some scholars have started to find solutions to quantify *COLREGs* [39], [40]. Second, regarding technological solutions, CA operation can be divided into a sequence of minor tasks, including situation awareness, risk assessment, strategy planning, and control execution [41]. In practice, the first two minor tasks, situation awareness and risk assessment, are usually merged as a complete problem set called *collision risk assessment* (*CRA*). Usually, this CRA is achieved by establishing different models for the collision risk index. The popular metrics used for CRA are distance (between the OS and TS) at the closest point of approach (DCPA) and time to the closest point of approach (TCPA) [42]. Aside from the metrics, a number of advanced algorithms have been developed for CRA, including the ship domain analysis [43], concept of the artificial potential field [44], velocity obstacles algorithm [45], and so forth. For CA path planning and control, there are traditional solutions, such as the line-of-sight [46] and other rule-based algorithms [47], while recently. as ship intelligence development thrives on machine learning, evolutionary [48], neural network solution [49], and reinforcement learning algorithms [50], [51] have also been introduced to solve CA problems.

We establish the concept of NPs to provide a quantitative guidance solution on the crossing CA operation.

We particularly focus on the importance of leveraging expertise wisdom, and collect, interpret, and conclude the human navigators' operational data to construct the concept and the derived solution for guidance support.

Methodology

In this section, we introduce the methodology of our research, which includes encounter situation setup, a description of the simulator (experiment) environment and data sources, the relevant calculated metrics used in NPA, and design of the guidance-support system. The simulator environment is illustrated in Figure 1, and two important issues, namely, the NPA and design of the guidance-support system, are presented in subflowcharts in Figure 1. The details of these two issues are introduced later in the "Experiment 1: NPA" and "Experiment 2: Guidance-Support System Testing" sections.

Encounter Situation

We investigate the crossing CA operation in a narrow strait as the research object. Three different ship encounter scenarios according to *COLREGs* are demonstrated in Figure 2, among which, our research interest lies in TS_1, where the TS is the stand-on vessel, and the OS must take actions to prevent potential risks. We adopt this scenario to address the pragmatic industrial engineering problem that exists in many heavy-traffic straits at sea.

In Figure 3, shown are two candidate paths when the OS encounters the TS. According to *COLREGs* Rule 15 Crossing Situation, the OS should alter its course to the starboard side to make a detour and pass behind the stern of the TS:

> Rule 15 Crossing Situation: When two power-driven vessels are crossing so as to involve risk of collision, the

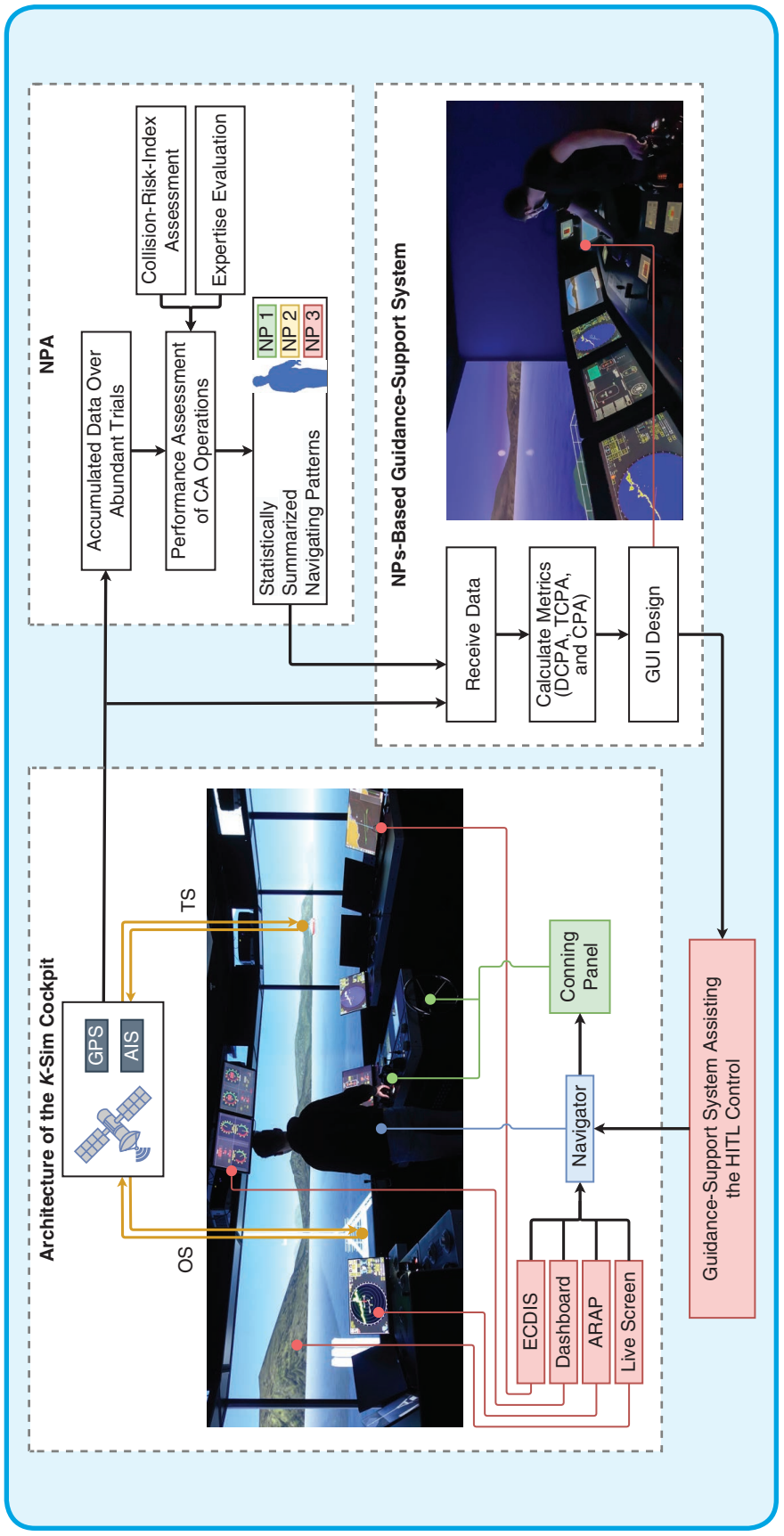

FIG 1 The workflow of this research work. HITL: hardware in the loop.

vessel which has the other on her own starboard side shall keep out of the way and shall, if the circumstances of the case admit, avoid crossing ahead of the other vessel.

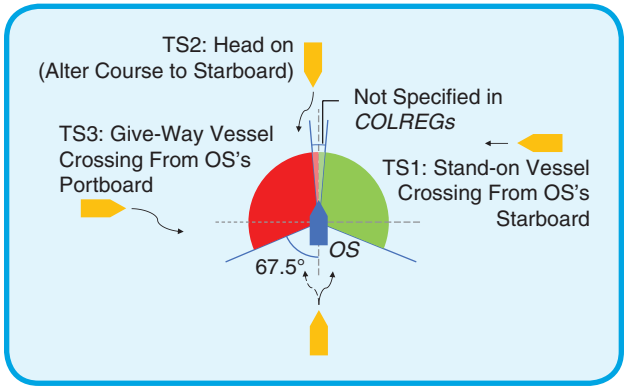

FIG 2 The three scenarios when an OS and TSs are in sight of one another, according to *COLREGs*.

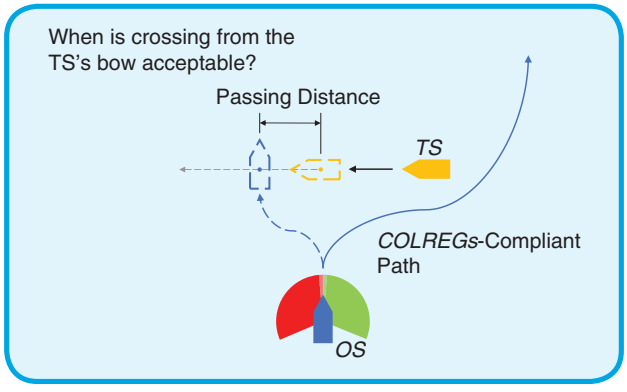

FIG 3 The path candidates when an OS encounters a TS from the starboard side.

Although *COLREGs* Rule 15 regulates its preference on who ought to be the stand-on/give-way vessel and on the corresponding operational requirements, it still reserves the possibility to let vessels violate the rule. In addition, from an industrial practice perspective, Rule 15 is deemed to be vague for actual operation. For instance, in busy strait water channels, if the OS sticks to the rule, it is barely possible for it to navigate across the strait when ships are coming from the starboard side in an endless stream. In this context, we attempt to quantify the metrics that describe a hierarchy of the maneuverable space, which enables the OS to pass from the bow of the starboard-side-coming TS and name them using different NPs.

Simulator Environment

The data used in this section are collected from a Kongsberg K-Sim maritime simulator, as shown in Figure 1 (Architecture of the K-Sim Cockpit). The simulator system can provide encoded GPS (for only the OS) and AIS (for both the OS and TS) data in standard forms starting with \$GP and \$AIVD, and the decoded data selected for the research goal in this section include

- from GPS: course, speed over ground, latitude and longitude (in WGS84), north and east (in UTM32N)
- from AISs: Maritime Mobile Service Identity, a series of nine digits, which is used to uniquely identify the ship, latitude and longitude (in WGS84), and course.

The positioning difference recorded in different coordinate systems, i.e., WGS84 and UTM32N, can be converted reciprocally. To make the calculation easier, we converted the longitude and latitude in WGS84 to north and east in UTM32N using the international unit meter.

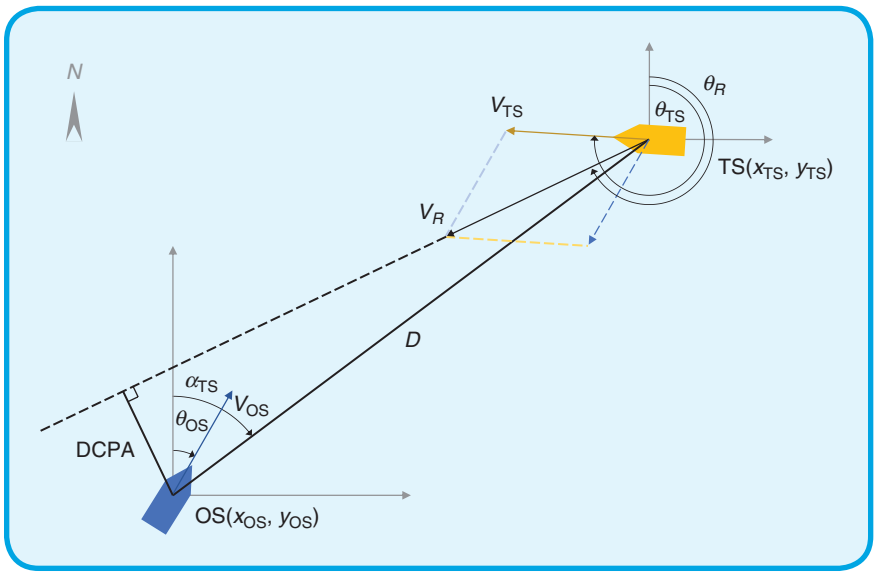

FIG 4 An illustration of DCPA.

Related Metrics

We use one of the most important collision risk indexes, DCPA, as the main criterion to assess NPs. The DCPA is a synthesis index capable of reflecting the motion properties of both the OS and TS [52]. It is illustrated in Figure 4 and calculated as

$$\mathrm{DCPA} = D \cdot \sin(\theta_R - \alpha_{TS}), \quad (1)$$

where D is the distance between the OS and TS, θ_R is the course of the relative velocity between the OS and TS, and α_{TS} is azimuth angle of the TS to the center of the OS (irrespective of the course of the OS).

Considering the collected data, (1) can be rewritten as

$$\begin{aligned}\mathrm{DCPA} &= D\cdot\sin(\theta_R-\alpha_{\mathrm{TS}})\\ &= D\cdot(\sin\theta_R\cdot\cos\alpha_{\mathrm{TS}}-\cos\theta_R\cdot\sin\alpha_{\mathrm{TS}})\\ &= D\cdot\left(\frac{V_{R,x}}{\|V_R\|}\cdot\frac{D_y}{D}-\frac{V_{R,y}}{\|V_R\|}\cdot\frac{D_x}{D}\right)\\ &= \frac{V_{R,x}}{\|V_R\|}\cdot D_y-\frac{V_{R,y}}{\|V_R\|}\cdot D_x,\end{aligned}\tag{2}$$

where V_R is the relative velocity between the OS and TS. The subscript x, y represent the projected component on the east and north directions, respectively.

Because the speed over ground (V_{OS}, V_{TS} for the OS and TS, respectively) and course angle ($\theta_{\mathrm{OS}}, \theta_{\mathrm{TS}}$ for the OS and TS, respectively) are collected, $V_R(V_{R,x}, V_{R,y})$ can be calculated as

$$\begin{aligned}V_{R,x} &= V_{\mathrm{TS},x}-V_{\mathrm{OS},x}\\ &= V_{\mathrm{TS}}\sin\theta_{\mathrm{TS}}-V_{\mathrm{OS}}\sin\theta_{\mathrm{OS}},\end{aligned}\tag{3}$$

$$\begin{aligned}V_{R,y} &= V_{\mathrm{TS},y}-V_{\mathrm{OS},y}\\ &= V_{\mathrm{TS}}\cos\theta_{\mathrm{TS}}-V_{\mathrm{OS}}\cos\theta_{\mathrm{OS}}.\end{aligned}\tag{4}$$

Based on the positions of the OS and TS, $D(D_x, D_y)$ can be calculated as

$$\begin{aligned}D_x &= x_{\mathrm{TS}}-x_{\mathrm{OS}},\\ D_y &= y_{\mathrm{TS}}-y_{\mathrm{OS}}.\end{aligned}\tag{5}$$

Taking (3)–(5) into (2), the DCPA can then be obtained.

In addition to the DCPA, the passing distance is calculated for further interpretation. The passing distance is briefly illustrated as in Figure 3. Comparing Figures 4 and 5, we can infer that the concept of the passing distance is more concise for the intuitive comprehension. Different from the DCPA, which serves as a capable index for collision prediction by exploiting the kinetics information of the OS and TS, the conceptual of the passing distance can be leveraged as an index candidate for the result-oriented assessment. There is not a general definition given to the passing distance, so in this article it is defined, specifically for the crossing CA situation, as

- *passing distance*: when two vessels are in a crossing CA close-encounter situation, the distance when one vessel first passes the velocity vector line of the other from the bow is defined as the *passing distance*.

According to the definition, passing distance is illustrated in Figure 5. It is imperative to figure out the moment t_{passing} when one vessel first passes the other. The offset from the OS to the velocity vector of the TS, $e_{\mathrm{OS}}^{\mathrm{TS}}$, can be calculated as

$$\begin{aligned}\hat{y}_{\mathrm{OS}} &= x_{\mathrm{OS}}\cdot\cot\theta_{\mathrm{TS}}+(y_{\mathrm{TS}}-x_{\mathrm{TS}}\cdot\cot\theta_{\mathrm{TS}}),\\ e_{\mathrm{OS}}^{\mathrm{TS}} &= \left|(\hat{y}_{\mathrm{OS}}-y_{\mathrm{OS}})\cdot\cos\theta_{\mathrm{TS}}\right|;\end{aligned}\tag{6}$$

while the offset from the TS to the velocity vector of the OS, $e_{\mathrm{TS}}^{\mathrm{OS}}$, can be calculated as

$$\begin{aligned}\hat{y}_{\mathrm{TS}} &= x_{\mathrm{TS}}\cdot\cot\theta_{\mathrm{OS}}+(y_{\mathrm{OS}}-x_{\mathrm{OS}}\cdot\cot\theta_{\mathrm{OS}}),\\ e_{\mathrm{TS}}^{\mathrm{OS}} &= \left|(\hat{y}_{\mathrm{TS}}-y_{\mathrm{TS}})\cdot\cos\theta_{\mathrm{OS}}\right|.\end{aligned}\tag{7}$$

Because x_{OS} and x_{TS} can be regarded as functions of time t, the passing moment t_{passing} can be calculated as

$$\min t_{\mathrm{passing}},\ \text{s.t. } e_{\mathrm{OS}}^{\mathrm{TS}}<\varepsilon_{\mathrm{OS}}\ \text{or}\ e_{\mathrm{TS}}^{\mathrm{OS}}<\varepsilon_{\mathrm{TS}},\tag{8}$$

where $\varepsilon_{\mathrm{OS}}$ and $\varepsilon_{\mathrm{TS}}$ are small values and shall be determined according to the vessels' velocities and the sampling frequencies in practice. And the distance between the OS and TS at t_{passing} is denoted as passing distance d_{passing}.

To design a guidance-support system, in addition to DCPA and passing distance, we calculated another two items: the TCPA and the coordinates of the CPA for the corresponding TSs.

The TCPA is calculated as

$$\begin{aligned}\mathrm{TCPA} &= D\cdot\frac{\cos(\theta_R-\alpha_{\mathrm{TS}})}{\|V_R\|}\\ &= D\cdot\frac{(\cos\theta_R\cdot\cos\alpha_{\mathrm{TS}}+\sin\theta_R\cdot\sin\alpha_{\mathrm{TS}})}{\|V_R\|}\\ &= \frac{\left(\frac{V_{R,y}}{\|V_R\|}\cdot D_y+\frac{V_{R,x}}{\|V_R\|}\cdot D_x\right)}{\|V_R\|},\end{aligned}\tag{9}$$

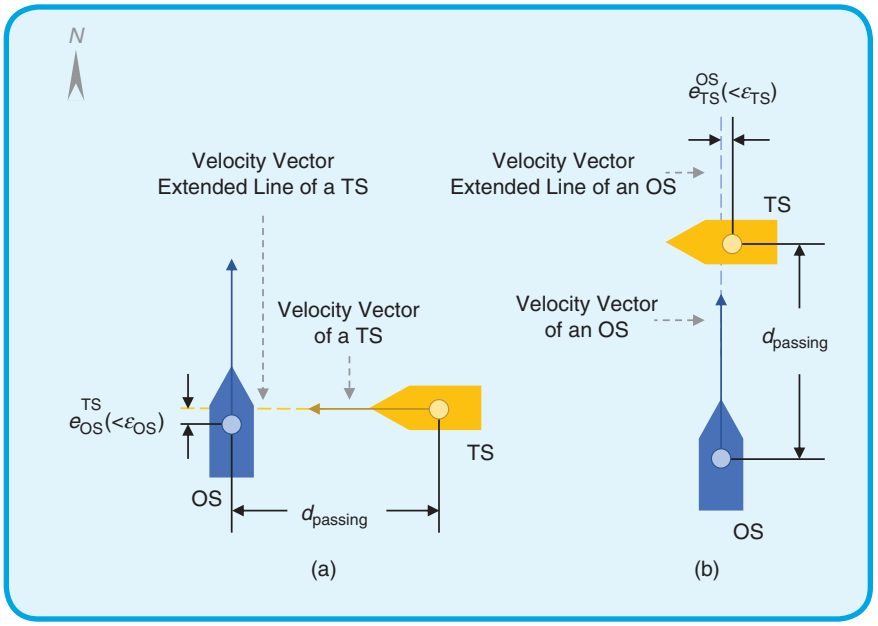

FIG 5 An illustration of the calculation of the passing distance at t_{passing}. (a) An OS passing from the bow of a TS and (b) a TS passing from the bow of an OS.

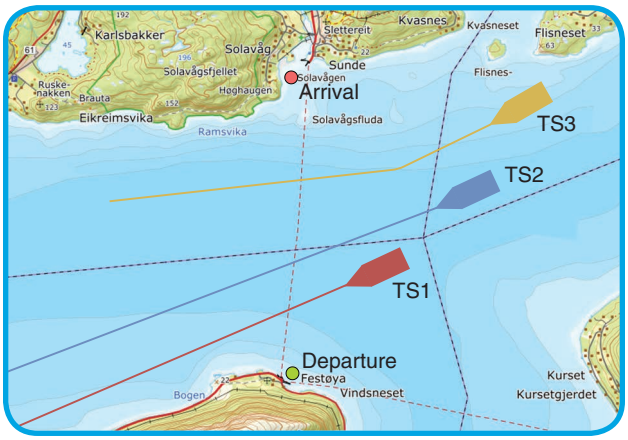

FIG 6 A scenario layout of the experimental CA sailing.

Table 2. Ship information and experimental conditions setup.

Property	OS	TS1	TS2	TS3
Basic information about ships				
Length (m)	88	133	165	170
Beam (m)	13.8	19.4	27.1	27.5
Initial states				
Heading (°)	312	245	245	240
Latitude (°)	62.3802	62.3882	62.3986	62.4031
Longitude (°)	6.3328	6.3357	6.3569	6.3443
Speed (knots)	0	14	15	10

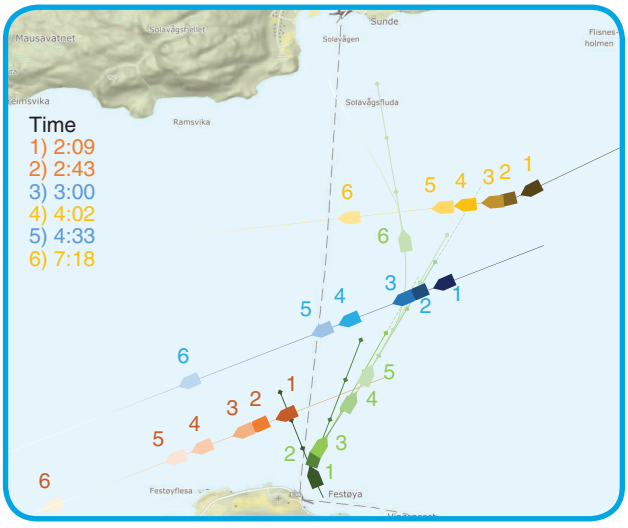

FIG 7 An example of a sea chart (trial F4R2B2, CA scheme: S-S-S).

The coordinate of the CPA $(x_{\text{CPA}}, y_{\text{CPA}})$ is calculated as

$$\begin{aligned} x_{\text{CPA}} &= x_{\text{OS}} + \text{TCPA} \cdot V_{\text{OS},x}, \\ y_{\text{CPA}} &= y_{\text{OS}} + \text{TCPA} \cdot V_{\text{OS},y}. \end{aligned} \tag{10}$$

Experiment 1: NPA

In this experiment, we deal with problems related to how NPs can be conceptualized by collectible data. In general, we attempt to seek the navigators' maneuvering logic and laws that are concealed in the data, and conclude different NPs. The significance of this section lies in two aspects: improving onboard decision support for the human-in-the-loop (HITL)-level MASS from an expertise perspective and developing ship intelligence by rationalizing the use of data, for instance, how they should be labeled.

Experiment Setup and Implementation

The water channel between two ports, Solavågen and Festøya in the Ålesund area of Norway, is selected as the basis for the simulation scene. The TSs in the simulation are named *TS1*, *TS2*, and *TS3*, and all of them come from the starboard side of the OS. The scenario construction is depicted in Figure 6. As a result, the simulator-based sailing task for the OS can be regarded as a complete sailing task comprising three sub-CA tasks with different encounter details, as listed in Table 2. The experiment implementation is carried out on K-Sim simulators at the Norwegian University of Science and Technology, Norwegian Maritime Competence Center in Ålesund. We collected 36 total trial sailings, and the trials are labeled in the form of 'F_R_B_' ('_' is a digit), where "F" means the experiments take place in February, while the digit following F represents the date; "R" denotes round, and the digit following R represents the round number; and "B" is an abbreviation for bridge, and the digit following B represents the bridge's serial number. For example, F4R2B2 means that the trial takes place on 4 February in round 2 and on bridge number 2.

Pattern Analysis

In this part of the experiment, we inspect and visualize the collected data, discuss the performance in each trial and how the collision risk index reflects the risk awareness w.r.t. the expertise perspective, and attempt to set up the clues that can sketch NPs.

CA Navigating Schemes

In the 36 trials, navigators took five different CA navigating schemes when they managed to complete the trial with multiple TSs. Passing from the bow of the TS is denoted as B, while passing from the stern of the TS is denoted as S. Then the five schemes are S-B-B, S-S-S, S-S-B, B-S-S, and B-B-B, and they appear in 19, 11, three, one, and two trials (out of 36), respectively. Theoretically, there can be another three schemes, including B-B-S, B-S-B, and S-B-S, but navigators do not choose to complete the task in these schemes. It is inferred that these schemes lead to odd paths that are neither efficient nor safe. The F4R2B2 trial, with the S-S-S scheme, is plotted in Figure 7. In the

chart, the footprints of six moments are detached. A vector line starting from the center of the OS with three markers indicates the predicted position in 1, 2, and 3 min in the current course direction. Each sub-CA task w.r.t. each TS corresponds to two footprints, one and two for TS1, three and five for TS2, and four and six for TS3. The first footprint of each sub-CA task points to the moment when the OS/TS passes the velocity vector of the TS/OS, i.e., the moment of passing (the moment when the passing distance is achieved), while the second footprint of each points to the moment when the OS arrives at the CPA. So Figure 7 demonstrates the detail of the trial that

- at 2:09, TS1 passes the velocity vector of the OS
- at 2:43, the OS arrives at the CPA w.r.t. TS1
- at 3:00, TS2 passes the velocity vector of the OS
- at 4:02, TS3 passes the velocity vector of the OS
- at 4:33, the OS arrives at the CPA w.r.t. TS2
- at 7:18, the OS arrives at the CPA w.r.t. TS3.

It is interesting to find that TS3 passes the OS before the OS arrives at the CPA with TS2. This is due to the definition of passing distance as the passing is deemed to have happened as long as one vessel has passed the velocity vector of the other. Therefore, although the OS is far from reaching TS3 at 4:02, due to the course alternation operation on the OS, TS3 passes the OS passively. Nevertheless, we cannot conclude that the CA subtask is over. As the OS restores its course to the direction of the destination, the collision risk may arise again. While in this situation, although the collision risk may re-emerge, there is a low possibility for it to happen. In this scenario where the TS has passed the OS, navigators usually chase the stern of the TS instead of immediately altering the course and heading to the destination and will steadily alter the course, directing to the destination after the collision risk is totally revoked.

The DCPA and passing distance w.r.t. the three TSs in F4R2B2 are presented in Figure 8. The figure shows that the passing moment under the passing distance definition (in Figure 5) can happen at very early stage, even when the OS is still far away from the TS. From the human's perspective, when navigators see that the TSs have passed the OS from the course direction, they have a sense of low collision risk.

Expert Evaluation

The 36 trials, which include 108 sub-CA tasks in total, are evaluated by experienced navigators rather than the navigators themselves. Three different evaluation levels are established to rate the CA performance. During the evaluation, the three levels labeled with green, yellow, and red colors, are used to mark the CA performance, as no specific terminology is yet created. According to navigators, the different evaluation levels can be intuitively described as

- *green*: the OS is operated to pass the TS at an ample distance; if passing from the bow, this distance enables the stand-on vessel to actively take action to avoid CA in some emergencies (such as OS engine failure). Meanwhile, passing in this level usually requires sparse operations on the OS control.
- *yellow*: the OS is operated to pass the TS at a sufficient distance with a certain degree of critical operations.
- *red*: the OS is operated to pass the TS at a tight distance, and the navigator needs to maneuver the vessel meticulously to safely pass the TS. If passing from the bow, sometimes such a pattern may provoke the operators of the TS.

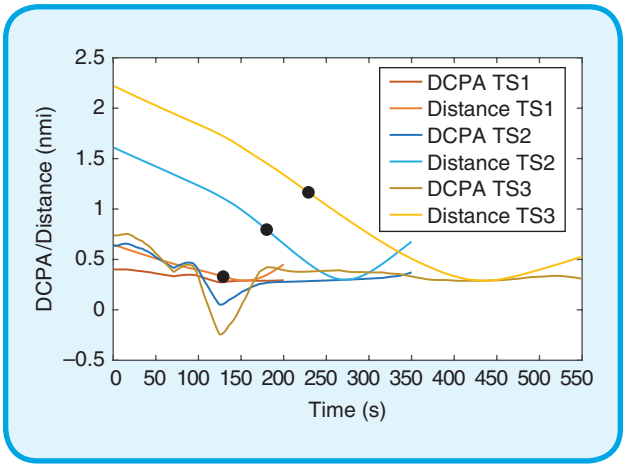

FIG 8 DCPA and distance to different TSs of the sea trial F4R2B2 in Figure 7. The black dots on curves of Distance TS_ represent data points at the passing moments.

The evaluation results are listed in Table 3. The table shows that a navigator may change his navigating strategies (the evaluation colors) in different subtasks.

- In CA with TS1, the OS passes TS1 from the bow in only three trials and all of them are rated red. In this task, the velocity of the OS has not been developed. Its initial course is in accordance with the quay infrastructure, which also decreases the maneuvering feasibility of the OS at the beginning stage. In this case, passing from the bow of TS1 becomes an adventurous strategy.
- In CA with TS2, the OS passes TS2 from the bow in 21 trials and from the stern in 15 trials. None of the 21 trials passing from the bow in this subtask is rated with the green label, while five trials taking the S-B-B CA scheme are rated with the red label. Passing TS1 from the stern detains the navigator to alter the course of the OS in the direction of passing TS2 from the bow. While in the 15 trials passing from the stern of TS2, three are rated green, eight are yellow, and four are red. For the three green trials, they are rated green in the CA with TS1 as well. For the four red trials, their DCPA in the preceding subtask are also at a low level in comparison with trials 20–27 and 31–33. However, it can be inferred that navigators are more flexible in choosing the strat-

Table 3. An expert evaluation on each CA and its information.

		TS1			TS2			TS3			
	Trial number	Evl.	DCPA (nmi)	$d_{passing}$ (nmi)	Evl.	DCPA (nmi)	$d_{passing}$ (nmi)	Evl.	DCPA (nmi)	$d_{passing}$ (nmi)	$d_{OS}^{arrival}$ (nmi)
S-B-B*											
1	F4R3B1		0.211	0.266		0.221	0.318		0.27	0.409	0.642
2	F4R3B2		0.181	0.235		0.251	0.396		0.403	0.612	0.583
3	F4R4B2		0.161	0.222		0.321	0.413		0.533	0.626	0.403
4	F5R1B4		0.175	0.252		0.265	0.367		0.529	0.619	0.352
5	F5R2B2		0.159	0.266		0.251	0.358		0.456	0.585	0.251
6	F5R3B2		0.149	0.256		0.341	0.441		0.536	0.638	0.346
7	F5R3B4		0.164	0.241		0.256	0.346		0.553	0.632	0.374
8	F5R4B2		0.151	0.25		0.331	0.411		0.513	0.634	0.298
9	F5R4B4		0.195	0.29		0.246	0.331		0.547	0.614	0.39
10	F4R4B1		0.174	0.224		0.245	0.356		0.379	0.52	0.528
11	F5R1B3		0.155	0.231		0.265	0.371		0.351	0.526	0.327
12	F5R2B1		0.183	0.231		0.206	0.281		0.249	0.352	0.568
13	F5R3B1		0.176	0.219		0.221	0.327		0.219	0.322	0.621
14	F5R4B3		0.131	0.201		0.222	0.343		0.349	0.459	0.231
15	F4R4B3		0.237	0.28		0.179	0.226		0.308	0.4	0.673
16	F4R2B1		0.202	0.252		0.161	0.258		0.221	0.316	0.624
17	F4R5B3		0.162	0.274		0.151	0.22		0.351	0.44	0.193
18	F4R5B4		0.112	0.181		0.201	0.34		0.321	0.428	0.173
19	F5R2B3		0.119	0.195		0.191	0.322		0.386	0.487	0.324
S-S-S											
20	F4R2B2		0.29	0.329		0.29	0.795		0.29	1.165	0.618
21	F5R2B4		0.322	0.351		0.292	0.712		0.308	0.951	0.684
22	F5R3B3		0.282	0.34		0.342	0.823		0.208	1.11	0.473
23	F5R1B2		0.222	0.334		0.142	0.343		0.308	0.323	1.158
24	F4R5B2		0.192	0.29		0.172	0.346		0.278	0.556	0.839
25	F5R1B1		0.287	0.326		0.176	0.256		0.141	0.22	0.857
26	F4R3B4		0.292	0.355		0.15	0.263		0.171	0.296	0.743
27	F4R2B3		0.19	0.262		0.19	0.501		0.2	0.704	0.598
28	F5R4B1		0.237	0.3		0.099	0.168		0.118	0.231	0.737
29	F4R5B1		0.222	0.281		0.088	0.145		0.09	0.14	0.734
30	F4R3B3		0.202	0.277		0.08	0.158		0.091	0.181	0.73
S-S-B											
31	F4R1B1		0.175	0.217		0.146	0.234		0.3	0.411	0.747
32	F4R1B4		0.07	0.125		0.111	0.172		0.428	0.519	0.623
33	F4R4B4		0.152	0.25		0.11	0.382		0.171	0.194	0.401
B-S-S											
34	F4R2B4		0.18	0.22		0.04	0.044		0.152	0.313	1.038
B-B-B											
35	F4R1B2		0.18	0.241		0.291	0.588		0.7	1.002	0.398
36	F4R1B3		0.12	0.185		0.301	0.502		0.65	0.92	0.31

*S denotes passing from the stern of the TS. B denotes passing from the bow of the TS.

egy when operating the OS to pass from the stern of the TS.

- In CA with TS3, the OS passes TS3 from the bow in 24 trial and from the stern in 12 trials. When passing from the bow, 11 trials are rated green, 11 yellow, and two red; when passing from the stern, six trials are rated green, five yellow, and one red. The evaluation distribution in two passing strategies are similar. The two red cases in which the OS passes from the stern reveal a strong peculiarity on the NPs of navigators as in the preceding subtask they also chose to pass from the stern of the TS tightly.

In accordance with the expertise evaluation results and their assessment principles, we renamed the color schemes with the terminology of the NPs: the green, yellow, and red colors stand for conservative, moderate, and aggressive modes, respectively.

DCPA Features

As the terminology of NPs, including conservative, moderate, and aggressive, are proposed, we consequently investigate the mapping between the patterns and the metrics (the DCPA and passing distance). Figure 9 depicts the DCPA distribution in terms of different NPs when passing from the stern and the bow separately. In the conservative pattern, passing from the stern and the bow have their medians around 0.289 and 0.533, and the distributed intervals (0.210, 0.340), (0.403, 0.553); in the moderate pattern, the medians are 0.160 and 0.268, and the intervals are (0.110, 0.202), (0.206, 0.386); in the aggressive pattern, the medians are 0.088 and 0.175, and the intervals are (0.040, 0.099), (0.120, 0.201).

From the distribution and the featured indexes, the following two facts can be found:

- The DCPA values selected by navigators to maneuver the OS at are distinctly different between passing from the stern and from the bow, regardless of the NPs. From the collected data, the median of DCPA values for passing from the bow are 1.84, 1.68, and 1.99 times for passing from the stern in the conservative, moderate, and aggressive pattern separately; the minimums are 1.92, 1.87, and 3.00 times; the maximums are 1.62, 1.91, and 2.03 times.
- The DCPA values between different patterns are clearly scattered on different scales, i.e., the DCPA can reveal the NPs to a certain extent.

Table 4 provides the mean DCPA values of passing from the stern/bow in each subtask. Thee table shows that the DCPA is less influenced by the CA-scenario difference in encounters with different TSs when passing from the stern, while the mean DCPA inclines to be larger when passing from the bow than from the stern. When passing from the stern, navigators prefer keeping the vessel to the original sailing route (without TSs on the route) as close as possible to achieve the least deviation and detour from the original route. To accomplish this, navigators usually keep a moderate speed to the course direction pointing to the stern of the TS. And once the TS passes, navigators alter the course back to the stern of the next TS, or directly to the destination (if no more CA operation is needed for another TS). This results in the insignificant difference in mean DCPA values between CA tasks with different TSs. When passing from the bow, the OS speed varies when it encounters different TSs. When it encounters TS1, the OS speed is low and developing; when it encounters TS2, it is moderate and still developing; when it encounters TS3, it is fully developed. It can be inferred that navigators choose to operate the OS at a larger DCPA to reduce the risk caused by the high-speed passing from the bow of the TS.

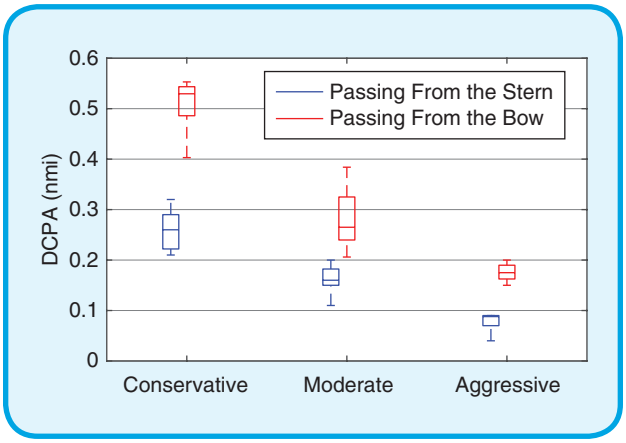

FIG 9 The distribution of DCPA in terms of different NPs.

Table 4. The mean DCPA for CA with different TSs.

Passing from	TS1	TS2	TS3
Stern	0.191	0.161	0.197
Bow	0.16	0.242	0.405

Note: The unit of values is nautical miles.

Passing Distance $d_{passing}$

Based on the data in Table 3, we calculate $d_{passing}$/DCPA values accordingly, and the results are plotted in Figure 10. The x-axis is divided into five intervals in terms of navigating schemes (see Table 3). The most important fact concluded from Figure 10 is that all the values are greater than one, i.e., $d_{passing}$ is always greater than the DCPA. From the definition of $d_{passing}$, we know that it is strictly the distance when one ship passes the center line (extended) of another. A $d_{passing}$/DCPA of greater than one means that the strict passing distance is always larger than the principal-metric DCPA. This guarantees that the DCPA is eligible as a CRA candidate for designing a guidance-support system in the

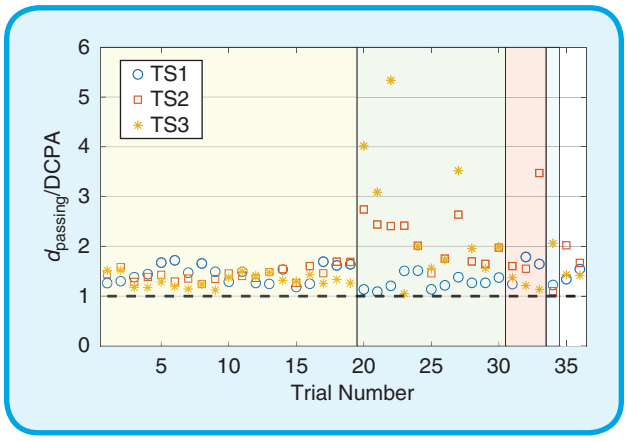

FIG 10 A plot of $d_{passing}$/DCPA values. The five intervals on the *x*-axis are S-B-B, S-S-S, S-S-B, B-S-S, and B-B-B; they are painted with distinguishable background colors.

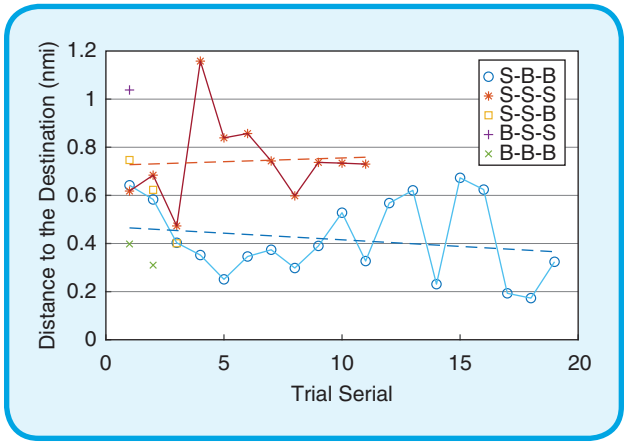

FIG 11 The distance to the destination at T = 550 s. The dashed lines in both red and blue are the trend lines of data sets S-S-S and S-B-B, respectively.

Table 5. DCPA scales of different NPs.

Passing from	Aggressive	Moderate	Conservative
Stern	<0.1	[0.1, 0.2)	≥ 0.2
Bow	<0.2	[0.2, 0.4)	≥ 0.4

Note: The unit of values is nautical miles.

next step, which means as long as the DCPA is selected in a proper way, $d_{passing}$ is secured.

Distance to the Destination $d_{OS}^{arrival}$

To investigate the efficiency of different CA schemes and NPs, the distance to the destination at T=550 s is calculated and listed in Table 3 and depicted in Figure 11. Considering that the OS has finished the CA subtasks with all the three TSs before T=550 s in all the trials, it is a proper time for efficiency assessment.

In terms of different CA schemes, most trials select S-B-B or S-S-S as the CA scheme, and other types are so rarely selected that they are not discussed statistically during this part of the experiment. From the figure, it can be seen that the distance to the destination is farther in general when the S-S-S scheme is selected. The S-S-S scheme means that the OS operated strictly under the CA operational requirements according to *COLREGs*, while the S-B-B scheme means that the OS only follows *COLREGs* in the first CA subtask and violates *COLREGs* in the remaining two subtasks. It can be inferred that the violation of *COLREGs* is the goal of increasing sailing efficiency; this is a tradeoff made by the navigator between efficiency and safety.

However, violating *COLREGs* makes maneuvering demanding for navigators. Comparing trials 16–18, although their strategies seem to be similar according to the classified patterns, the real situation might be to the contrary. Choosing the S-B-B scheme requires navigators to take proper maneuvering commands at very appropriate moments: passing the TS1 from the stern at an ample but close distance and then altering the heading to pass the TS2 from the bow once the collision risk with TS1 is canceled. If the navigator does not alter the heading at the correct time, he/she might be caught in a situation of parallel racing with TS2 to pass from its bow. This may result in a long-distance detour from the designed route, as in trials 15 and 16. In summary, if navigators take very proper operations at the correct time, taking an aggressive strategy may shorten the sailing time (as in trials 17 and 18), but if proper operations are not taken at the right time, the endeavor might be in vain.

From Table 3, the trials are listed in order based on the NPs, from safe to risky in each scheme. Nonetheless, from the curves in Figure 11, we cannot locate a trend of how the efficiency can be affected by the NPs, which also proves that maneuvering the OS in a risky manner may be in vain when it comes to increasing sailing safety.

Summary

In this section, we collect and analyze data from a one-direction multi-TSs CA scenario that imitates the traffic-separation scheme in the Dover Strait water channel. Based on the calculation of key-metrics DCPA and the expertise evaluation upon scenario reconstruction, we concluded three different NPs in terms of the DCPA for passing the TS from the stern and the bow separately. In addition to the DCPA, we use two additional calculated figures—the passing distance and the distance to the destination (at T = 550 s)—to comprehensively interpret navigators' rationality in CA operations. Finally, we concluded the DCPA scales for the different patterns in Table 5.

Another important factor drawn from the collected data is that there is no evidence for any relationship between sailing efficiency and the NPs in a complete sailing. But

the CA scheme, i.e., the path routing, has a significant effect on efficiency. That is, a conclusion on NPs will support navigators in regulating ship maneuvering and enhancing their judgment on path routing. Understanding NPs helps to reduce the possibility of entering a collision-risky zone. It also prevents the OS from deviating far from the original route.

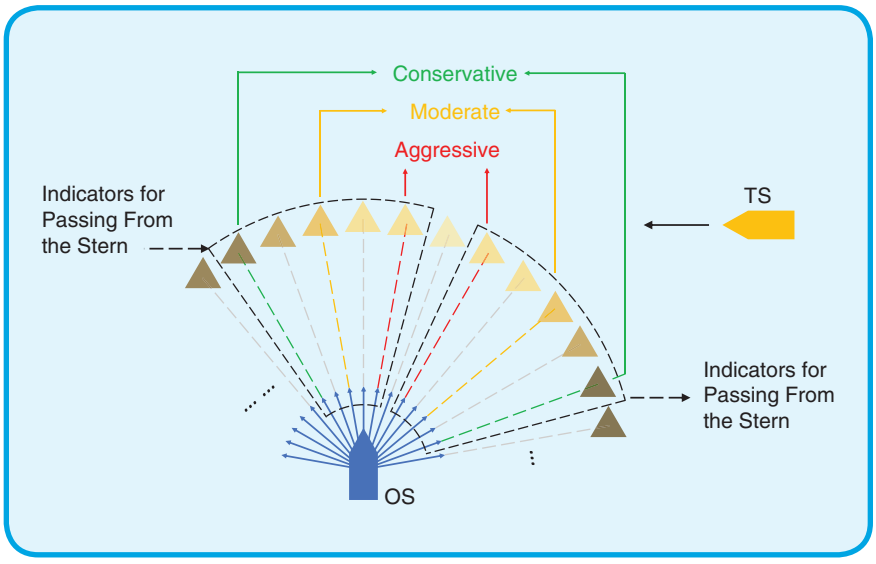

FIG 12 An illustration of the GUI of the developed system.

Experiment 2: Guidance-Support System Testing

In this section, we develop a real-time onboard decision-support system for human-centered navigation based on the NPA results from the "Experiment 1: NPA" section. The aims of developing such a system are

- for onboard decision support, especially in the seafarers' training program as it has been reported that students in the nautical training think *COLREGs* is difficult to understand [18] as it is stated in the "Summary" section of "Experiment 1: NPA" that understanding the NPA can potentially enhance navigators' judgment on path routing.
- for the development of ship intelligence in the framework of MASS shown in Table 1, specifically for MASS at the HITL level. In the current ECDIS and ARPA systems, there is very limited information about planning and prediction, which means navigators need to calculate alternatives and deploy navigation strategies by him or herself. In this respect, the system developed in this section offers an innovative supplementary solution to the ECDIS.

Description of the Guidance-Support System

The guidance-support system is developed to support navigators in making decisions in the CA scenario. Similar to the existing ECDIS, the system to be developed should be concise, informative, and functional. To be concise, it requires that no irrelevant information are shown on the GUI, which helps navigators focus on key elements. To be informative, it requires the GUI to provide as much information as possible in a wise manner. To be functional, it requires the system to be easily understood for decision making and operation reacting at navigators' favors.

Taking the calculated items as the basis, a GUI of the navigating support system is developed and illustrated in Figure 12. The steps to form this GUI are

- The DCPA at the current position and speed is calculated but with different courses. The range of the course is before the center of the OS (–90°, 90°), and the step is 1°.
- Among the calculated DCPA, the ones with smallest offsets with the values of the NPs are selected to be the indicators for the course in the GUI. And the course lines with red, yellow, and green indicate aggressive, moderate, and conservative NPs, respectively, accordingly. The raw calculated DCPA values can be either positive or negative, with the positive implying that the OS passes the TS from the bow and the negative suggesting that the OS passes the TS from the stern. Therefore, it is easy to distinguish these two NPs in terms of passing from the stern/bow when sketching the GUI.
- For the rest of the calculated DCPA, the TCPA and CPA are calculated at a step of 5°, and the CPA are then drawn on the GUI with triangles in different color depths. The OS tends to encounter a more dangerous situation if it is navigated in the direction of a lighter-colored triangle.

The developed system is updated once new AIS/GPS data from the OS and the TSs are received.

Validation on Simulator and Statistical Analysis

The developed system is validated in four trials in the same scenario as in the "Methodology" section on the simulator. Among these trials, the S-B-B CA scheme is selected in two trials, the S-S-S and B-B-B CA schemes are chosen in one trial each.

The key features of the testing trials are listed in Table 6. Regarding NP selection, it can be found that with the developed system, in all four trials, the OS is navigated to pass the TS in the moderate pattern in 15 subtasks and one in the conservative pattern (according to its DCPA and the definition given in the "Experiment 1: NPA" section). We may conclude that the system has a positive performance

in assisting the navigator to take a moderate pattern to navigate the OS. Considering the distance to the destination, the performance in the S-B-B CA scheme trials (MR1-2) is at an average level compared with the trials in Table 3; in the trial (MR3) taking the S-S-S scheme, it is at a low level, which means that the efficiency is high; and in the trial (MR4) taking B-B-B scheme, it is higher than the trials in Table 3. Comparing MR4 with the F4R1B2-3 trials in Table 3: The NP when passing TS1 is changed from aggressive to moderate, and it can be deemed a result of balancing efficiency and safety.

Table 6. The test results with the developed system.

	TS1		TS2		TS3		
Trial number	NP	DCPA	NP	DCPA	NP	DCPA	$d_{OS}^{arrival}$
S-B-B							
MR1		0.142		0.285		0.297	0.517
MR2		0.133		0.237		0.281	0.345
S-S-S							
MR3		0.239		0.146		0.117	0.574
B-B-B							
MR4		0.203		0.328		0.394	0.494

Note: The unit of values is nautical miles.

Illustration of an Example Case

In this part of the experiment, we take the MR2 trial as an example to see how the developed guidance-support system can assist the navigator with taking preventive actions in CA operations. We took three screenshots from the GUI of the guidance-support system during the trial, and the screenshots of the OS at this moment are deemed to be critical for CA operations. The screenshots are presented in Figure 13, and the exact times and descriptions of each moment are explained.

In Figure 13(a), the OS has finished the CA operation with TS1, and it depicts that the OS is navigated in a direction between the red and yellow lines, which represent aggressive and moderate patterns, respectively. Comparing with Figure 13(b), it can be seen that the navigator keeps the direction unaltered since the moment in Figure 13(a). Finally, the OS passes the TS2 with a DCPA at 0.237 nmi in a moderate pattern, as displayed in Table 6.

After the OS finishes the CA operation against the TS2, the navigator starts to alter the course. Figure 13(c) indicates that the OS passes over the CA with TS2 and

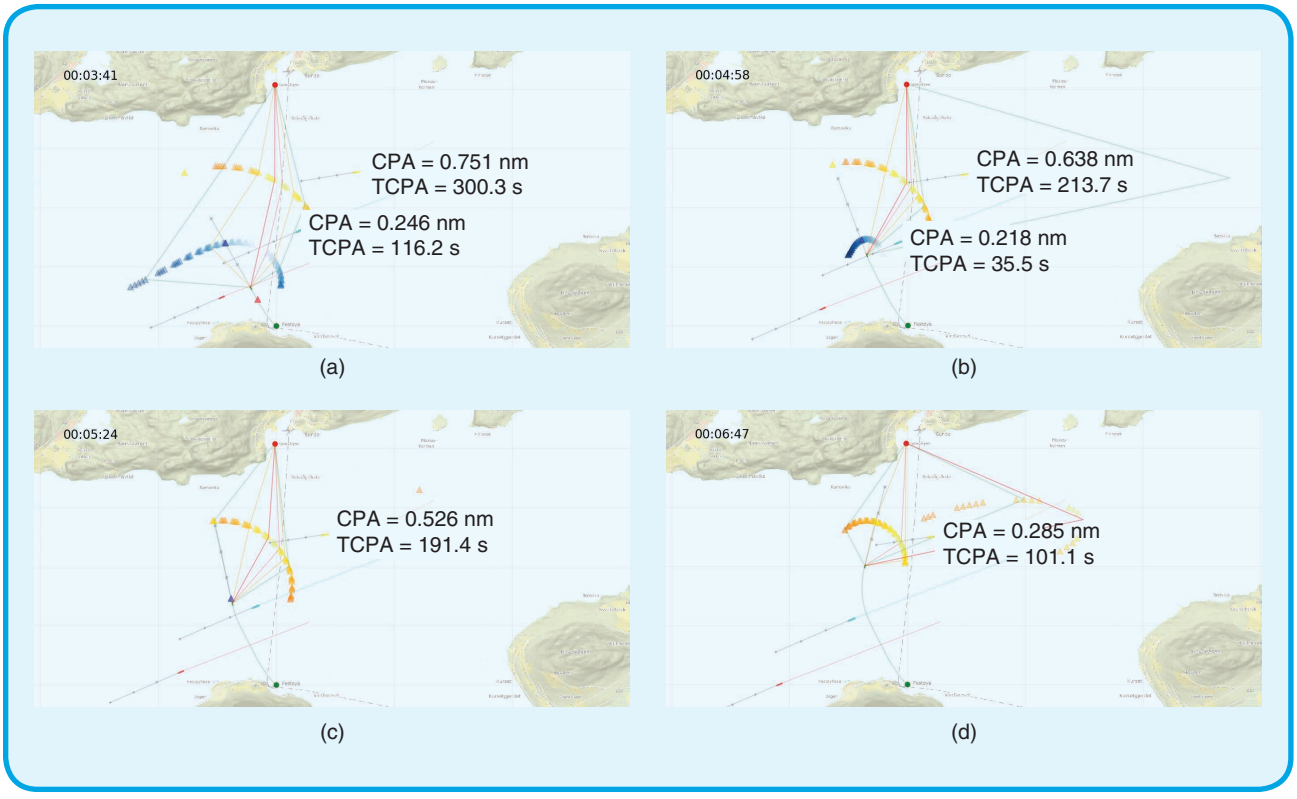

FIG 13 Screenshots of the guidance-support system for some critical moments from trial MR2. (The CPA text indicator in this figure represents the DCPA as this is to keep in accordance with the ARPA system and the navigators' conventions. The TCPA remains its denotation.) (a) At 00:03:41, CA with TS1 is finished; CA with TS2 is underway. (b) At 00:04:58, an OS is passing the velocity vector extended line of TS2. (c) At 00:05:24, CA with TS2 is finished; CA with TS3 is underway. (d) At 00:06:47, CA with TS3 is underway.

begins to make a back turn toward the destination. At this moment, the guidance-support system shows that if the OS keeps the current course, it will pass the TS3 in a conservative pattern. However, the navigator plans to balance the efficiency under the instruction of the system so that the navigator gradually alters the course until the moment in Figure 13(d), when the OS has been switched in a direction identified as moderate. Comparing Figure 13(c) and (d), it is clear that sailing efficiency is promoted. Furthermore, as the support system suggests that the direction in Figure 13(d) is moderate, the navigator does not need to worry about any collision risk in this case.

Summary (Part Two)

From the statistical analysis and the realization of an example, we conclude that the developed system has a positive influence on navigators' navigating manners. It reduces the navigators' brainwork on calculation and planning of the sailing route to some extent by providing some indicating information.

Limitations and Future Work

The study of navigators' operational behaviors is essential for the development of MASS. This research work makes an attempt to describe it using the concepts of NP and NPA, and the concepts are established in a quantitative approach in terms of collision risk index DCPA. The limitations of this research mainly include that the metrics for NPA rely only on the collision risk index, which may not completely describe navigators' behavioral profiles, and the scenario setup considers only the crossing CA situation.

In the next stage, we will address these two aspects. The first is to establish a complete monitoring system and take more potential and influential factors into account, such as, brain electrical activities [53], [54] and eye movement [55], which may reflect navigators' attention, so that we can obtain a sketch of their NPs with extended details. The second aspect is to collect more data in different scenarios, including other CA situations as well as other critical ship-maneuvering scenarios, such as docking. All the planned work is designed to better understand the navigating logic of human navigators in the hopes of shedding light on both the development of MASS and human–machine-interaction performance as MASS is still at the HITL level.

Conclusion

In this article, we aimed to solve the pragmatic industrial issues of maritime traffic that are often found in narrow water channels. We proposed and conceptualized NPs of navigators and designed a scenario that imitates the traffic situation as an attempt to find the best navigation solution. Through simulator-based experiments, we collected 36 trials' data for analyzing NPs. Three NPs, namely aggressive, moderate, and conservative modes, were classified with the help of expertise knowledge from experienced navigators. They were further quantified for CA tasks in terms of the DCPA, an imperative collision risk index. Based on detected NPs, a guidance-support system with GUI was developed for a one-direction multiship CA scenario. The developed system was also tested on the simulator, and its performance on guidance support was assessed to be positive from the test results. The research approach used in this article is the first one that conceptualizes and quantifies NPs and subsequently develops their importance on industrial applications in the maritime industry.

Acknowledgment

The research is supported, in part, by the MAROFF KPN project "Digital Twins for Vessel Life Cycle Service" (project number 280703), and in part by the IKTPLUSS Project's "Remote Control Centre for Autonomous Ship Support" (project number 309323) in Norway. We extend our gratitude to Knut Remøy for his help in organizing experiments.

About the Authors

Baiheng Wu (baiheng.wu@ntnu.no) earned his M.Sc. degree in marine cybernetics from Norwegian University of Science and Technology (NTNU), Trondheim, Norway. He is currently pursuing his Ph.D. degree as a member of the Intelligent Systems Laboratory, Department of Ocean Operations and Civil Engineering, with NTNU, Ålesund, 6009, Norway. His research interests extend to control theory, optimization, and machine learning algorithms and their applications in the maritime industry. He is a Student Member of IEEE.

Guoyuan Li (guoyuan.li@ntnu.no) earned his Ph.D. degree in computer science from the Department of Informatics, Institute of Technical Aspects of Multimodal Systems, University of Hamburg, Germany. He is currently a professor of ship intelligence with the Intelligent Systems Laboratory, Department of Ocean Operations and Civil Engineering, Norwegian University of Science and Technology, Ålesund, 6009, Norway. His research interests include the modeling and simulation of ship motion, autonomous navigation, intelligent control, optimization algorithms, and locomotion control of bioinspired robots. He is a Senior Member of IEEE.

Luman Zhao (luman.zhao@ntnu.no) earned her Ph.D. degree at the Department of Naval Architecture and Ocean Engineering, Seoul National University, Korea. She is currently a postdoctoral research associate as a member of the Intelligent Systems Laboratory, Department of Ocean Operations and Civil Engineering, Norwegian University of Science and Technology, Ålesund, 6009, Norway. Her research interests include autonomous ship maneuvering, deep reinforcement learning, hardware-in-the-loop simulation, and optimization.

Hans-Ingar Johansen Aandahl (hiaandah@stud.ntnu.no) earned his professional certificate of Competency Deck Officer Class 3. He earned his bachelor's degree in nautical science in the Department of Ocean Operations and Civil Engineering, Norwegian University of Science and Technology, Ålesund, 6009, Norway, where he serves as the teaching assistant for a series of navigation courses. His research interests include maritime transportation, marine traffic, and navigators' behavioral analysis.

Hans Petter Hildre (hans.p.hildre@ntnu.no) earned his Ph.D. degree from Norwegian University of Science and Technology, Trondheim, Norway. He is a professor and head of the Department of Ocean Operations and Civil Engineering, Norwegian University of Science and Technology, Ålesund, 6009, Norway. He is also the center director for the Centre for Research Driven Innovation within marine operations. His research interests include product design and system architecture design.

Houxiang Zhang (hozh@ntnu.no) earned his Ph.D. degree in mechanical and electronic engineering from Beihang University, Beijing, China. He is a full professor of mechatronics in the Department of Ocean Operations and Civil Engineering, Faculty of Engineering, Norwegian University of Science and Technology, Ålesund, 6009, Norway. He was elected a member of the Norwegian Academy of Technological Sciences. His research interests include control, optimization, and artificial intelligence applications, especially on autonomous vehicles; and marine automation, digitalization, and ship intelligence. He is a Senior Member of IEEE.

References

[1] Z. Pietrzykowski, "Maritime intelligent transport systems," in *Proc. Int. Conf. Transp. Syst. Telematics*, 2010, pp. 455–462.

[2] L. Chen, R. R. Negenborn, Y. Huang, and H. Hopman, "Survey on cooperative control for waterborne transport," *IEEE Intell. Transp. Syst. Mag.*, vol. 13, no. 2, pp. 71–90, 2020. doi: 10.1109/MITS.2020.3014107.

[3] K. Wróbel, J. Montewka, and P. Kujala, "Towards the assessment of potential impact of unmanned vessels on maritime transportation safety," *Rel. Eng. Syst. Safety*, vol. 165, pp. 155–169, Sept. 2017. doi: 10.1016/j.ress.2017.03.029.

[4] S. Fang, Y. Wang, B. Gou, and Y. Xu, "Toward future green maritime transportation: An overview of seaport microgrids and all-electric ships," *IEEE Trans. Veh. Technol.*, vol. 69, no. 1, pp. 207–219, 2019. doi: 10.1109/TVT.2019.2950538.

[5] E. Tu, G. Zhang, L. Rachmawati, E. Rajabally, and G.-B. Huang, "Exploiting AIs data for intelligent maritime navigation: A comprehensive survey from data to methodology," *IEEE Trans. Intell. Transp. Syst.*, vol. 19, no. 5, pp. 1559–1582, 2017. doi: 10.1109/TITS.2017.2724551.

[6] R. Skulstad, G. Li, T. I. Fossen, B. Vik, and H. Zhang, "Dead reckoning of dynamically positioned ships: Using an efficient recurrent neural network," *IEEE Robot. Automat. Mag.*, vol. 26, no. 3, pp. 39–51, 2019. doi: 10.1109/MRA.2019.2918125.

[7] M. Zhu, W. Sun, A. Hahn, Y. Wen, C. Xiao, and W. Tao, "Adaptive modeling of maritime autonomous surface ships with uncertainty using a weighted LS-SVR robust to outliers," *Ocean Eng.*, vol. 200, p. 107053, 2020. doi: 10.1016/j.oceaneng.2020.107053.

[8] Z. Liu, Y. Zhang, X. Yu, and C. Yuan, "Unmanned surface vehicles: An overview of developments and challenges," *Annu. Rev. Control*, vol. 41, pp. 71–93, 2016. doi: 10.1016/j.arcontrol.2016.04.018.

[9] International Maritime Organization. "Outcome of the Regulatory scoping exercise on maritime autonomous surface ships." IMO press release, MSC.1/Circ.1638, Annex, pp. 3–4, June 3, 2021

[10] "Maritime autonomous surface ships industry conduct principles & code of practice, a voluntary code, version 4," Maritime UK, 2020, pp. 19–20

[11] "DNVGL-CG-0264 class guideline: Autonomous and remotely operated ships," *DNVGL*, 2018.

[12] "LR code for unmanned marine systems," in *ShipRight Design and Construction, Additional Design Procedures*. Lloyd's Register, London, UK, 2017.

[13] Ø. J. Rødseth and H. Nordahl, "Definitions for autonomous merchant ships," *Norwegian Forum Unmanned Ships, Version*, vol. 1, pp. 7–10, Oct. 2017.

[14] F. Goerlandt, "Maritime autonomous surface ships from a risk governance perspective: Interpretation and implications," *Safety Sci.*, vol. 128, p. 104758, Aug. 2020. doi: 10.1016/j.ssci.2020.104758.

[15] G. Li, L. Yang, S. Li, X. Luo, X. Qu, and P. Green, "Human-like decision making of artificial drivers in intelligent transportation systems: An end-to-end driving behavior prediction approach," *IEEE Intell. Transp. Syst. Mag.*, early access, July 1, 2021. doi: 10.1109/MITS.2021.3085986.

[16] "Convention on the international regulations for preventing collisions at sea (COLREGS)," International Maritime Organization, London, UK, 1972.

[17] "Remote-controlled and autonomous ships position paper," DNVGL, 1363 Høvik, Norway, 2018.

[18] D. Ivanišević, A. Gundić, and D. Mohović, "Difficulties in understanding the COLREGS among the students from different systems of education for seafarers," *TransNav, Int. J. Marine Navigation Safety Sea Transp.*, vol. 13, no. 4, pp. 869–873, Dec. 2019.

[19] C. Livadas, J. Lygeros, and N. A. Lynch, "High-level modeling and analysis of the traffic alert and collision avoidance system (TCAS)," *Proc. IEEE*, vol. 88, no. 7, pp. 926–948, 2000. doi: 10.1109/5.871302.

[20] G. Zylius, "Investigation of route-independent aggressive and safe driving features obtained from accelerometer signals," *IEEE Intell. Transp. Syst. Mag.*, vol. 9, no. 2, pp. 103–113, 2017. doi: 10.1109/MITS.2017.2666583.

[21] G. Li, S. E. Li, B. Cheng, and P. Green, "Estimation of driving style in naturalistic highway traffic using maneuver transition probabilities," *Transp. Res. C, Emerg. Technol.*, vol. 74, pp. 113–125, Jan. 2017. doi: 10.1016/j.trc.2016.11.011.

[22] Z. Chen, Y. Zhang, C. Wu, and B. Ran, "Understanding individualization driving states via latent Dirichlet allocation model," *IEEE Intell. Transp. Syst. Mag.*, vol. 11, no. 2, pp. 41–53, 2019. doi: 10.1109/MITS.2019.2903525.

[23] G. Li et al., "Risk assessment-based collision avoidance decision-making for autonomous vehicles in multi-scenarios," *Transp. Res. C, Emerg. Technol.*, vol. 122, p. 102820, 2021. doi: 10.1016/j.trc.2020.102820.

[24] G. Li, Y. Chen, D. Cao, X. Qu, B. Cheng, and K. Li, "Extraction of descriptive driving patterns from driving data using unsupervised

algorithms," *Mech. Syst. Signal Process.*, vol. 156, p. 107589, Jan. 2021. doi: 10.1016/j.ymssp.2020.107589.

[25] Z. Li, L. Chen, C. Roberts, and N. Zhao, "Dynamic trajectory optimization design for railway driver advisory system," *IEEE Intell. Transp. Syst. Mag.*, vol. 10, no. 1, pp. 121–132, 2018. doi: 10.1109/MITS.2017.2776134.

[26] S. A. Shappell and D. A. Wiegmann, "The human factors analysis and classification system—HFACS," Federal Aviation Administration, U.S. Department of Transportation, Washington, D.C., Rep. DOT/FAA/AM-00/7, Feb. 2000.

[27] S.-T. Chen, A. Wall, P. Davies, Z. Yang, J. Wang, and Y.-H. Chou, "A human and organisational factors (HOFS) analysis method for marine casualties using HFACS-maritime accidents (HFACS-MA)," *Safety Sci.*, vol. 60, pp. 105–114, Dec. 2013. doi: 10.1016/j.ssci.2013.06.009.

[28] S. Yildiz, Ö. Uğurlu, J. Wang, and S. Loughney, "Application of the HFACS-PV approach for identification of human and organizational factors (HOFS) influencing marine accidents," *Rel. Eng. Syst. Safety*, vol. 208, p. 107395, Apr. 2021. doi: 10.1016/j.ress.2020.107395.

[29] P. Sotiralis, N. P. Ventikos, R. Hamann, P. Golyshev, and A. Teixeira, "Incorporation of human factors into ship collision risk models focusing on human centred design aspects," *Rel. Eng. Syst. Safety*, vol. 156, pp. 210–227, Dec. 2016. doi: 10.1016/j.ress.2016.08.007.

[30] T. Zhou, C. Wu, J. Zhang, and D. Zhang, "Incorporating cream and MCS into fault tree analysis of LNG carrier spill accidents," *Safety Sci.*, vol. 96, pp. 183–191, July 2017. doi: 10.1016/j.ssci.2017.03.015.

[31] M. J. Akhtar and I. B. Utne, "Human fatigue's effect on the risk of maritime groundings—a Bayesian network modeling approach," *Safety Sci.*, vol. 62, pp. 427–440, Feb. 2014. doi: 10.1016/j.ssci.2013.10.002.

[32] J. Zhao and W. Price, "A statistical study of mariners' behaviour in collision avoidance at sea," in *Proc. Int. Conf. Marine Simul. Manoeuvrabil. (MARSIM '96)*, M. S. Chislett Eds., Copenhagen, Denmark, Sept. 9–13, 1996, p. 169. 1996.

[33] T. Abramowicz-Gerigk and A. Hejmlich, "Human factor modelling in the risk assessment of port manoeuvers," *TransNav, Int. J. Marine Navig. Safety Sea Transp.*, vol. 9, no. 3, pp. 427–433, 2015. doi: 10.12716/1001.09.03.16.

[34] Z. Pietrzykowski, M. Wielgosz, and M. Breitsprecher, "Navigators' behavior analysis using data mining," *J. Marine Sci. Eng.*, vol. 8, no. 1, pp. 50, 2020. doi: 10.3390/jmse8010050.

[35] J.-B. Yim, D.-J. Park, and I.-H. Youn, "Development of navigator behavior models for the evaluation of collision avoidance behavior in the collision-prone navigation environment," *Appl. Sci.*, vol. 9, no. 15, p. 3114, 2019. doi: 10.3390/app9153114.

[36] R. Zghyer and R. Ostnes, "Opportunities and challenges in using ship-bridge simulators in maritime research," in *Proc. Ergoship 2019*, pp. 1–13, 2019.

[37] G. Li, R. Mao, H. P. Hildre, and H. Zhang, "Visual attention assessment for expert-in-the-loop training in a maritime operation simulator," *IEEE Trans. Ind. Informat.*, vol. 16, no. 1, pp. 522–531, 2019. doi: 10.1109/TII.2019.2945361.

[38] D.-J. Park, J.-B. Yim, H.-S. Yang, and C-k Lee, "Navigators' errors in a ship collision via simulation experiment in South Korea," *Symmetry*, vol. 12, no. 4, p. 529, 2020. doi: 10.3390/sym12040529.

[39] B.-O. H. Eriksen, G. Bitar, M. Breivik, and A. M. Lekkas, "Hybrid collision avoidance for ASVS compliant with COLREGS rules 8 and 13–17," *Front. Robot. AI*, vol. 7, p. 11, Feb. 2020. doi: 10.3389/frobt.2020.00011.

[40] K. Woerner, M. R. Benjamin, M. Novitzky, and J. J. Leonard, "Quantifying protocol evaluation for autonomous collision avoidance," *Autonom. Robots*, vol. 43, no. 4, pp. 967–991, 2019. doi: 10.1007/s10514-018-9765-y.

[41] R. Zaccone and M. Martelli, "A collision avoidance algorithm for ship guidance applications," *J. Marine Eng. Technol.*, vol. 19, no. sup1, pp. 62–75, 2020. doi: 10.1080/20464177.2019.1685836.

[42] L. Kang, Z. Lu, Q. Meng, S. Gao, and F. Wang, "Maritime simulator-based determination of minimum DCPA and TCPA in head-on ship-to-ship collision avoidance in confined waters," *Transp. A, Transp. Sci.*, vol. 15, no. 2, pp. 1124–1144, 2019. doi: 10.1080/23249935.2019.1567617.

[43] Z. Pietrzykowski and M. Wielgosz, "Effective ship domain–impact of ship size and speed," *Ocean Eng.*, vol. 219, p. 108423, 2021. doi: 10.1016/j.oceaneng.2020.108423.

[44] H. Lyu and Y. Yin, "Colregs-constrained real-time path planning for autonomous ships using modified artificial potential fields," *J. Navig.*, vol. 72, no. 3, pp. 588–608, 2019. doi: 10.1017/S0373463318000796.

[45] Y. Huang and P. Van Gelder, "Time-varying risk measurement for ship collision prevention," *Risk Anal.*, vol. 40, no. 1, pp. 24–42, 2020. doi: 10.1111/risa.13293.

[46] P. Wilson, C. Harris, and X. Hong, "A line of sight counteraction navigation algorithm for ship encounter collision avoidance," *J. Navig.*, vol. 56, no. 1, p. 111, 2003. doi: 10.1017/S0373463302002163.

[47] A. Savvaris, H. Niu, H. Oh, and A. Tsourdos, "Development of collision avoidance algorithms for the C-Enduro USV," *IFAC Proc. Vol.*, vol. 47, no. 3, pp. 12,174–12,181, 2014.

[48] G. Li, H. P. Hildre, and H. Zhang, "Toward time-optimal trajectory planning for autonomous ship maneuvering in close-range encounters," *IEEE J. Ocean. Eng.*, vol. 45, no. 4, pp. 1219–1234, 2019. doi: 10.1109/JOE.2019.2926822.

[49] J.-H. Ahn, K.-P. Rhee, and Y.-J. You, "A study on the collision avoidance of a ship using neural networks and fuzzy logic," *Appl. Ocean. Res.*, vol. 37, pp. 162–173, Aug. 2012. doi: 10.1016/j.apor.2012.05.008.

[50] L. Zhao and M.-I. Roh, "Colregs-compliant multiship collision avoidance based on deep reinforcement learning," *Ocean Eng.*, vol. 191, p. 106436, Nov. 2019. doi: 10.1016/j.oceaneng.2019.106436.

[51] H. Niu, Z. Ji, F. Arvin, B. Lennox, H. Yin, and J. Carrasco, "Accelerated sim-to-real deep reinforcement learning: Learning collision avoidance from human player," in *Proc. IEEE/SICE Int. Symp. Syst. Integrat. (SII)*, 2021, pp. 144–149. doi: 10.1109/IEEECONF49454.2021.9382693.

[52] Y. Hu, A. Zhang, W. Tian, J. Zhang, and Z. Hou, "Multi-ship collision avoidance decision-making based on collision risk index," *J. Marine Sci. Eng.*, vol. 8, no. 9, p. 640, 2020. doi: 10.3390/jmse8090640.

[53] T. G. Monteiro, C. Skourup, and H. Zhang, "Using eeg for mental fatigue assessment: A comprehensive look into the current state of the art," *IEEE Trans. Human-Machine Syst.*, vol. 49, no. 6, pp. 599–610, 2019. doi: 10.1109/THMS.2019.2938156.

[54] G. Li, W. Yan, S. Li, X. Qu, W. Chu, and D. Cao, "A temporal-spatial deep learning approach for driver distraction detection based on EEG signals," *IEEE Trans. Autom. Sci. Eng. (from July 2004)*, 2021. doi: 10.1109/TASE.2021.3088897.

[55] R. Mao, G. Li, H. P. Hildre, and H. Zhang, "A survey of eye tracking in automobile and aviation studies: Implications for eye-tracking studies in marine operations," *IEEE Trans. Human-Machine Syst.*, vol. 51, no. 2, pp. 87–98, 2021. doi: 10.1109/THMS.2021.3053196.

[56] Chen, H. et al., "From automation system to autonomous system: An architecture perspective," *J. Mar. Sci. Eng.*, vol. 9, no. 6, p. 645, 2021. doi: 10.3390/jmse9060645.

ITS